High Throughput Computational Framework of Materials Properties for Extreme Environments

PIs: Zi-Kui Liu [a], Allison M. Beese [a,b], and Shun-Li Shang [a]
Researchers: Adnan Eghtesad [a], John D. Shimanek [a], and Shuang Lin [a]

[a] Department of Materials Science and Engineering, Pennsylvania State University, University Park, PA 16802, USA
[b] Department of Mechanical Engineering, Pennsylvania State University, University Park, PA 16802, USA

PennState College of Earth and Mineral Sciences | Department of Materials Science and Engineering

Acknowledgment and Disclaimer

- This material is based upon work supported by the Department of Energy Award Number DE-FE0031553.

Outline

- Predictive crystal plasticity modeling of Ni single crystal based on first-principles calculations
- Density functional theory informed dislocation density hardening within crystal plasticity: Application to Ni polycrystals
- First-principles calculations of ideal shear strength for Ni-X-Z dilute multicomponent alloys

Overview of high throughput computational framework for materials properties under extreme environments

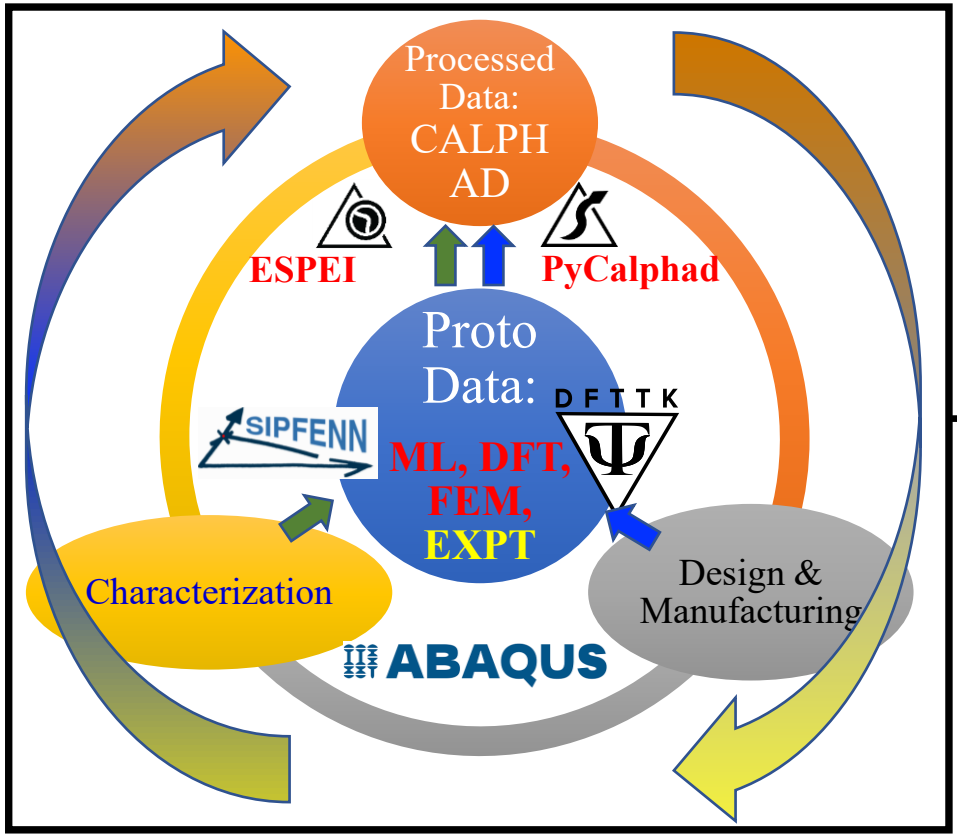

- Predict proto data using DFT Tool Kit (www.DFTTK.org) and machine learning models (https://phaseslab.com/sipfenn/)
- Apply FEM (ABAQUS) and dislocation density based FFT methods to predict tensile strain-stress curve
- Use CALPHAD approach (PyCalphad.org and ESPEI.org) to model processed data
- Validate results and improve models

Mechanical Behavior from First Principles

Physically-meaningful crystal plasticity parameters → predictive framework for deformation

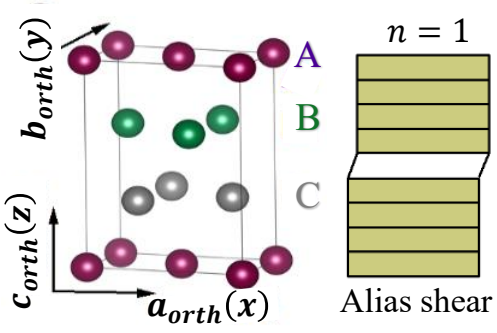

$$\dot{\tau}_c^{\alpha} = \sum_{\beta=1}^{l} h_{\alpha\beta}\left|\dot{\gamma}^{\beta}\right|$$

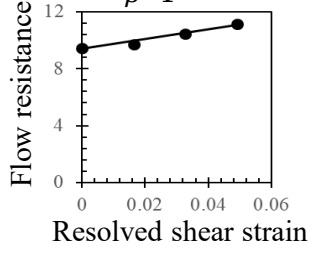

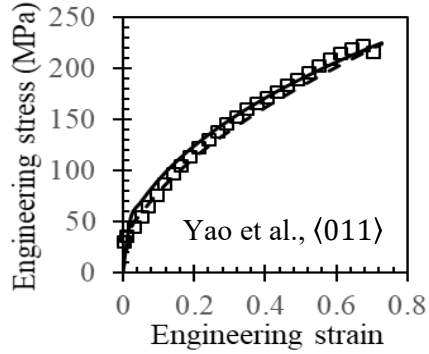

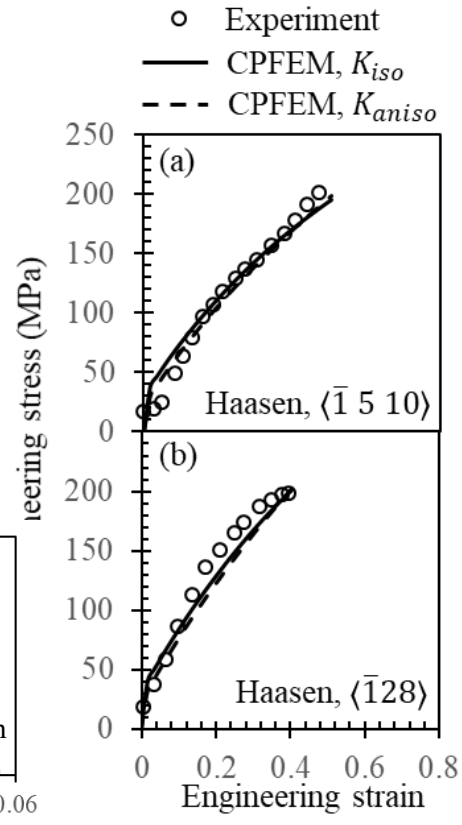

Atomic scale → **Mesoscale** → **Macroscale**

DFT-based predictions

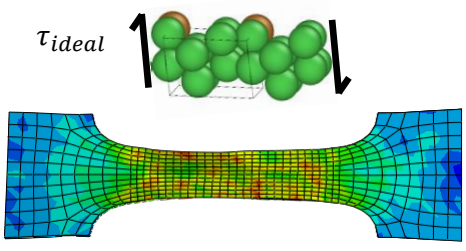

Slip system hardening

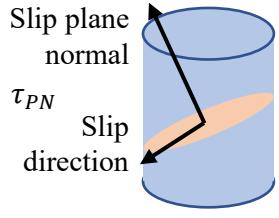

Crystal plasticity

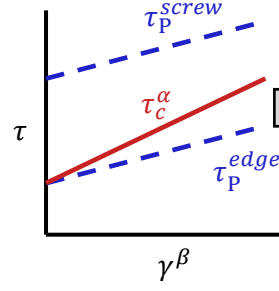

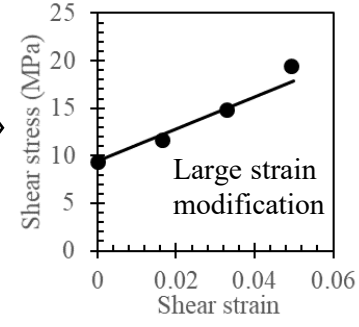

Shimanek et al. *JOM* 74 (2022) 1423-1434

First-Principles Calculations for Crystal Plasticity

- Elastic constants

- Ideal shear stress:

- Alias shear – one layer involved
- One lattice parameter fixed, all else relaxed
- Needs a conversion to dislocation-mediated critical resolved shear stress

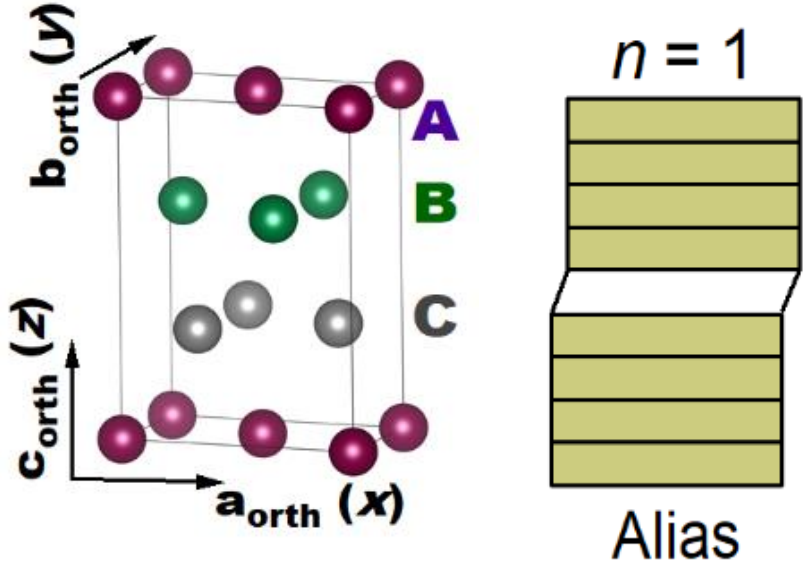

Joós-Duesbery Peierls-Nabarro model:

$$\tau_{\mathrm{P}} = \frac{Kb}{a}\exp\left(\frac{-2\pi Kb}{4\pi d\tau_{\mathrm{IS}}}\right)$$

τ_{IS}: Ideal shear strength from DFT-based calculations (a function of pre-strains)

K: anisotropic elastic factor, **which depends on dislocation character**

a, d: lattice periodicity length respectively within slip plane, between slip places

Joós and Duesbery, *Phys Rev Lett* 78: 266-9, 1997.

Describing Hardening at Finite Strain

Need to account for short range effects on dislocation motion – increased screw dislocation density within junctions with increase of strain

- Flow stress from $K^{edge} \rightarrow \tau_{\mathrm{P}}^{edge}$ (low)
- Flow stress from $K^{screw} \rightarrow \tau_{\mathrm{P}}^{screw}$ (high)

Low strains (edge dislocation behavior):

$$\tau_c^{\alpha} = \tau_{\mathrm{P}}^{edge}$$

Large strains (edge, screw, junction behavior):

$$\tau_c^{\alpha} = \left(1 - w\gamma^{\beta}\right)\tau_{\mathrm{P}}^{edge} + w\gamma^{\beta}\tau_{\mathrm{P}}^{screw}$$

w - Weighting factor (0.33, calibrated with macroscale experimental data from Yao et al.)

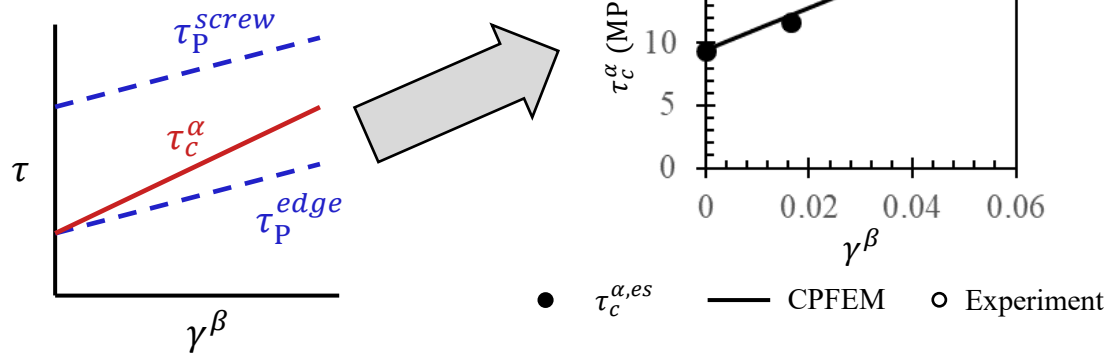

Shimanek et al. *JOM* 74 (2022) 1423-1434

Yao et al., *J. Nucl. Mater. 2003,* 323:2–3, 388– 393.

Experimental Comparison: Ni

- With accurate τ_0 & h_0, can calibrate τ_s
  - Based on Yao data (as is w) at one orientation
- Use these parameters to predict large strain response of new orientations:

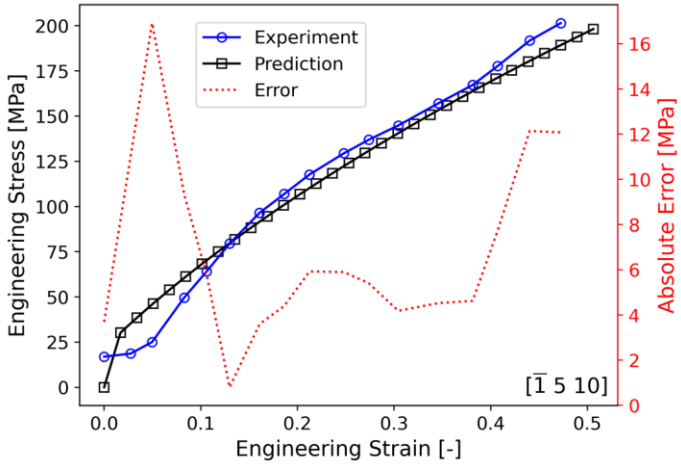

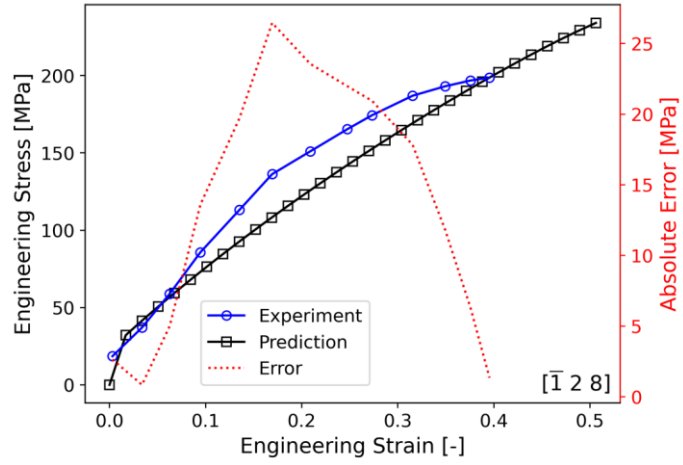

- $\tau_c^{\alpha,es}$ — CPFEM °Experiment

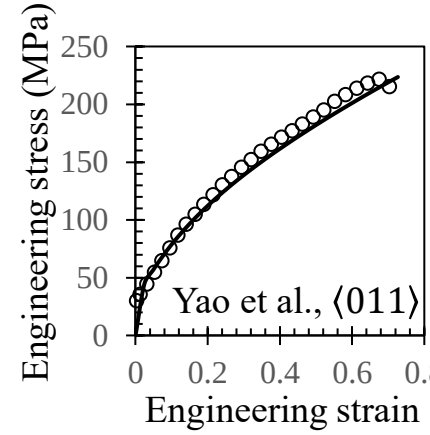

Reasonable agreement at large strains

Shimanek et al. *JOM* 74 (2022) 1423-1434

Haasen, *Philos. Mag. 1958,* 328, 384–418.
Yao et al., *J. Nucl. Mater. 2003,* 323:2–3, 388– 393.

Extension to Alloys: Binary Ni-X ($Ni_{11}X$)

- Alias shear deformation to Ni-X ($Ni_{11}X$) solution
- 26 alloying elements
- Use alloying element **descriptors** to examine the variations of ideal shear strength

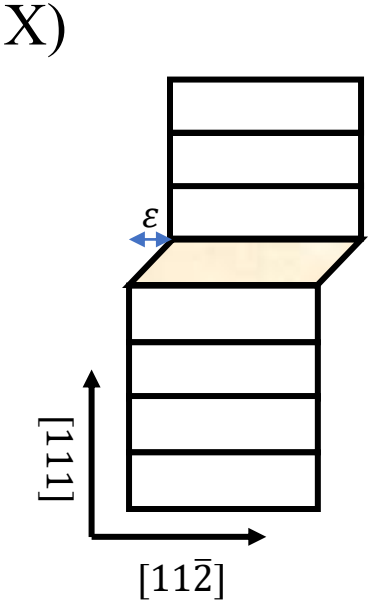

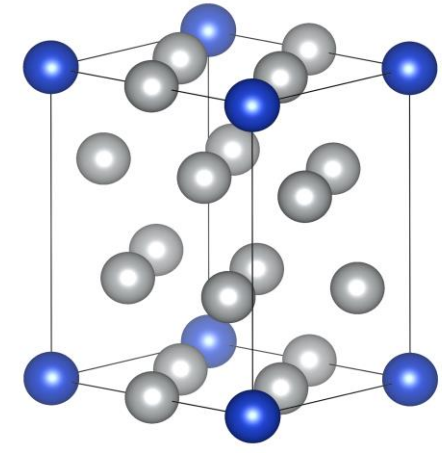

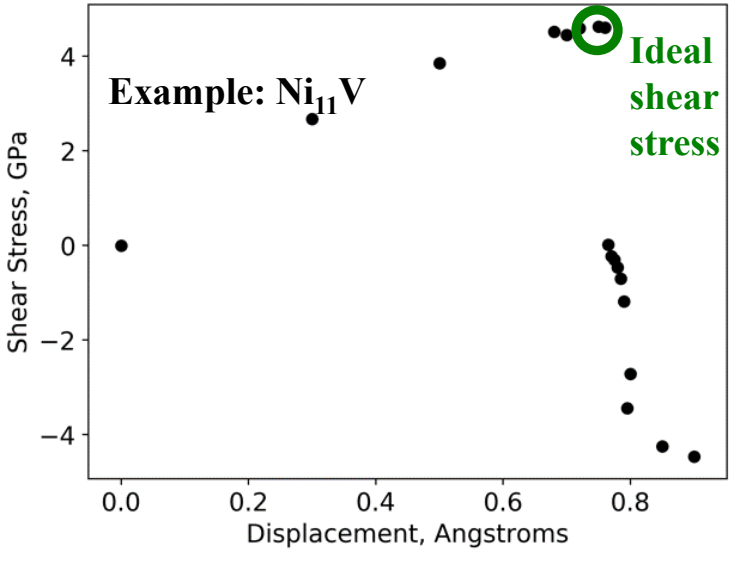

τ_{ideal}:

										13 Al	14 Si
21 Sc	22 Ti	23 V	24 Cr	25 Mn	26 Fe	27 Co	28 Ni	29 Cu	30 Zn	31 Ga	32 Ge
39 Y	40 Zr	41 Nb	42 Mo	43 Tc	44 Ru	45 Rh	46 Pd	47 Ag	48 Cd	49 In	50 Sn
71 Lu	72 Hf	73 Ta	74 W	75 Re	76 Os	77 Ir	78 Pt	79 Au	80 Hg	81 Tl	82 Pb

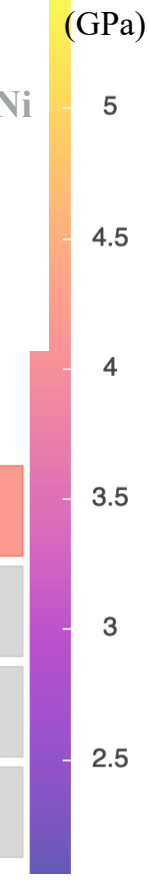

$Ni_{11}X$ Correlational Study

Index	Regression Relief Algorithm	Coefficient of Determination	Maximal Information Coefficient	Backward Wrapper: SVM	Forward Wrapper: SVM
1	Volume	Volume	Volume	Electronic conductivity	Volume
2	Electron Density	Electronegativity	Electronegativity	Volume	Debye Temperature
3	Mendeleev Number	Electron Density	Debye Temperature	No. F Valence Filled	G
4	Covalent Radius	Covalent Radius	E	Debye Temperature	Electronic Conductivity
5	Standard Entropy	Debye Temperature	G	Heat Capacity	No. F Valence Unfilled
6	Electronegativity	Pauling Electronegativity	Mendeleev Number	Electron Density	E
7	Pseudopotential Radius: s-shell	Mendeleev Number	Covalent Radius	Covalent Radius	Electronegativity
8	Pseudopotential Radius: p-shell	G	Electron Density	No. Valence Filled	Heat of Sublimation
9	Electron Range	E	No. D Valence Unfilled	No. P Valence Filled	B
10	Debye Temperature	No. Valence Unfilled	Group	Mass	Boiling Temperature

- 26 Ni-based binary alloys, 45 atomic features
- Shown are five measures of association between pure atomic physical features and calculated ideal shear strength
- Several features in common:
  - **Volume**
  - **Debye Temperature**
  - **Covalent radius**
  - **Electron density**
  - **Electronegativity**
- Unexpected is the low importance of elastic constants

arXiv: 2108.06412

Ternary Ni-X-Z ($Ni_{34}XZ$) Ideal Shear Stress

Strengthening elements

Softening elements

(Pure Ni_{36}: 5.10 GPa)

	Co	Mn	Fe	Cr	Al	Ti	Mo	Si	Nb
Co	5.24	5.20	5.18	5.10	4.98	4.86	4.81	4.83	4.62
Mn		5.17	5.17	5.07	4.92	4.82	4.76	4.71	4.57
Fe			5.15	5.05	4.92	4.82	4.77	4.73	4.57
Cr				4.84	4.86	4.70	4.64	4.73	4.48
Al					4.73	4.63	4.59	4.53	4.42
Ti						4.55	4.51	4.41	4.34
Mo							4.45	4.41	4.29
Si								4.31	4.17
Nb									4.16

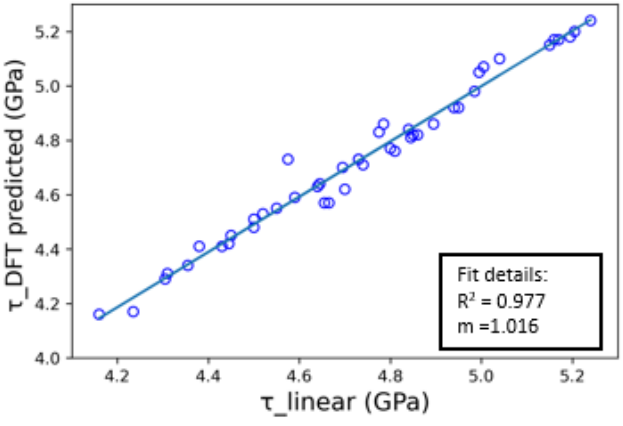

Deviation from fit above indicates nonlinear effects not captured in equation below:

$$\tau_{id}^{linear}(Ni_{34}XZ) = 0.5 * \tau_{id}(Ni_{34}X_2) + 0.5 * \tau_{id}(Ni_{34}Z_2)$$

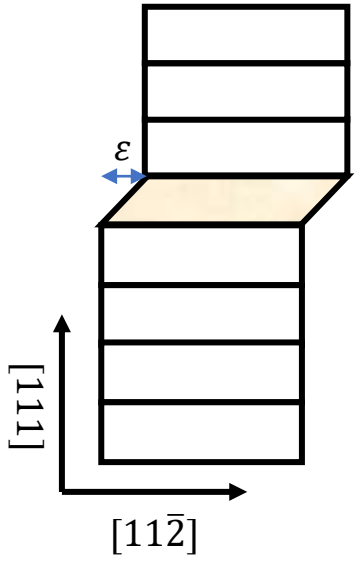

Alias shear deformation

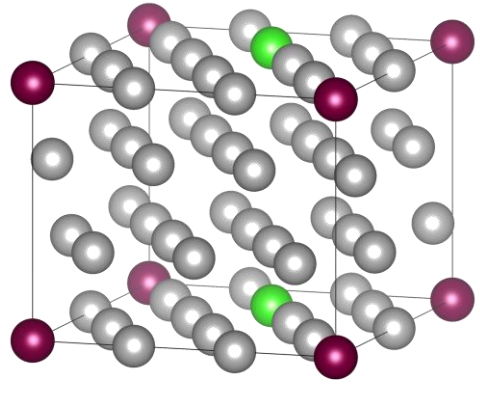

$Ni_{34}XZ$ Correlational Study

Index	Ftest	Regression Relief Algorithm	Coefficient of Determination	Maximal Information Coefficient
1	Volume	Volume	Volume	Volume
2	B_DFT	Van der Waals atomic radius	G/B_DFT	B_DFT
3	G/B_DFT	Boiling Temperature	Cohesive energy	Cohesive energy
4	Heat of Fusion	The third ionization potential	B_DFT	G/B_DFT
5	Cohesive energy	Elastic constant C12_DFT	Vaporization heat	Heat of Sublimation
6	Mass	Heat of Sublimation	Elastic constant C44_DFT	Poisson ratio
7	Heat of Sublimation	Cohesive energy	Heat of Sublimation	Mass
8	Number of valence electron	The first ionization potential	Poisson ratio	Heat of Fusion
9	Van der Waals atomic radius	Elastic constant C13_DFT	Number of valence electron	Square root of B/G
10	Vaporization heat	Heat of Fusion	Square root of B/G	Vaporization heat

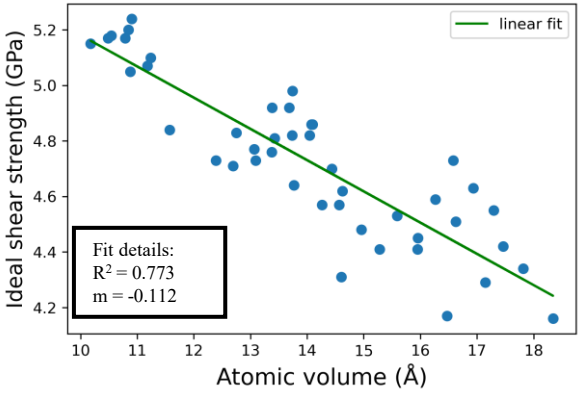

- 45 Ni-based ternary alloys, 80 physical features
- Several features in common:
  - Volume (agree with Ni-X study)
  - Ratio between shear modulus and bulk modulus
  - Cohesive energy
  - Bulk modulus
  - Vaporization heat

Extension of PAN-CPFEM to Polycrystals

1. Simplified polycrystal microstructures:

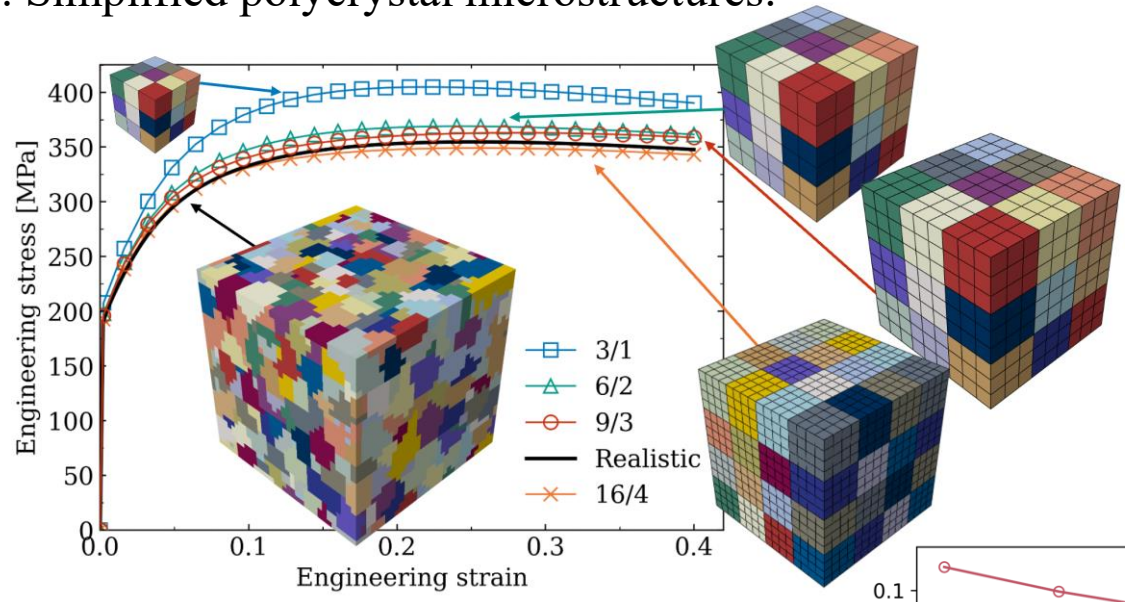

2. Automated parameter optimization:

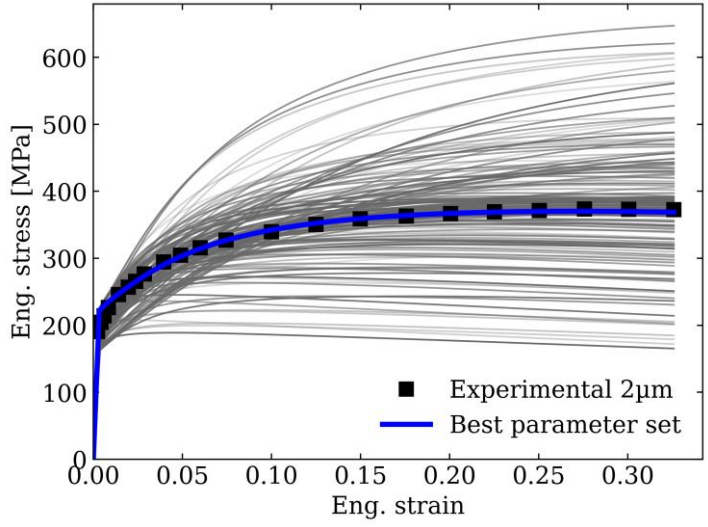

3. Grain size dependence shows power law behavior for all hardening parameters.

Exponent varies with material, may correlate with material properties such as stacking fault energy (shown to right).

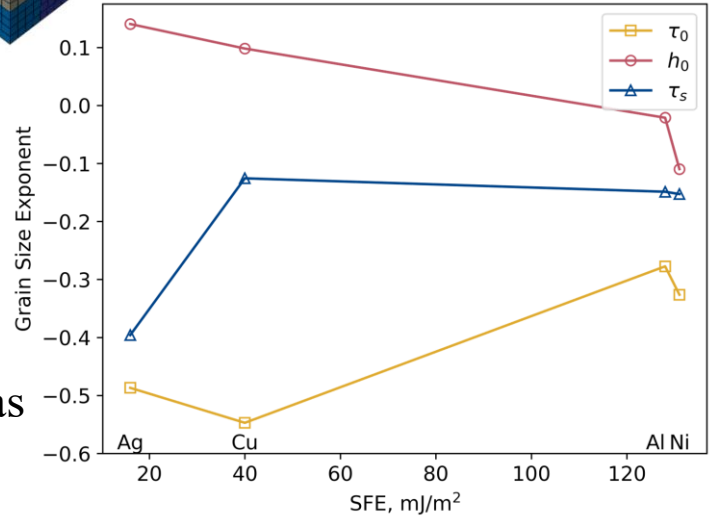

4. Slow performance and unclear physical interpretations motivates move from CPFEM using PAN to FFT using dislocation density hardening law

Crystal plasticity fast Fourier transform (CPFFT)

CPFFT explicitly models the microstructure, individual grains, slip systems and their interactions to capture the micromechanical anisotropy of polycrystals

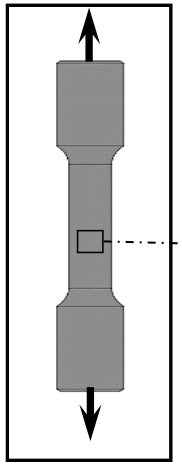

Tensile test

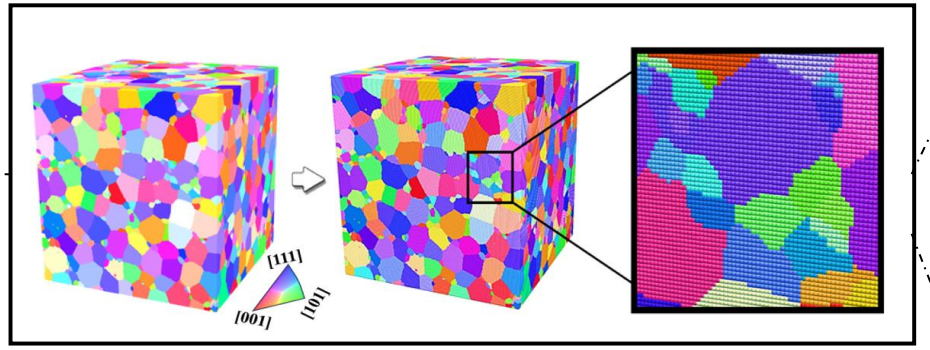

Microstructure

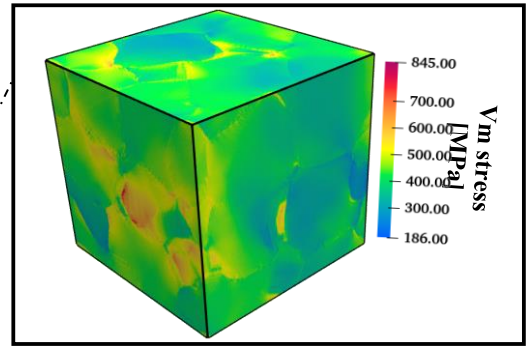

Full-field

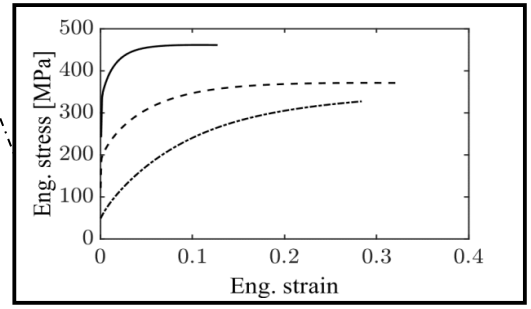

Flow response

High-performance CPFFT

~400x speed up on 10 Tesla V100 GPUs

Orders of magnitude faster than CPFEM

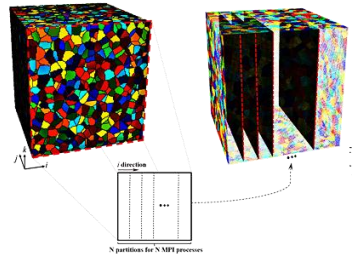

Domain decomposition of material microstructure for hybrid Multi-CPU/GPU accelerated simulation

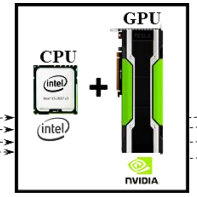

GPU plus CPU per computing node

Supercomputer with computing nodes of GPU and CPU

Original dislocation density (DD) hardening

$$\tau_c^s = \tau_0^s + \tau_{for}^s + \tau_{deb}$$

$$\tau_{0,HP}^s + \tau_{0,for}^s$$

$$0.9\mu b\sqrt{\rho_{for}^s + 1.05\sum_{s\neq s'}\rho_{for}^{s'}}.$$

$$0.086\,\mu b\sqrt{\rho_{deb}}\,\log\left(\frac{1}{\sqrt{\rho_{deb}}}\right)$$

$$\frac{H_{HP}\mu\sqrt{b}}{\sqrt{d_{mfp}^{grain}}}$$

$$\tau_{for}^s\big|_{t=0}$$

$$\frac{\partial\rho_{for}^s}{\partial\gamma} = k_1\sqrt{\rho_{for}^s} - k_2\rho_{for}^s$$

$$\frac{\partial\rho_{deb}}{\partial\gamma} = \left[q\sum_s b\sqrt{\rho_{deb}}\,k_2\right]\rho_{for}$$

$$\frac{2}{\sqrt{\frac{\hat{b}_x^{s\,2} + \hat{b}_y^{s\,2} + \hat{b}_z^{s\,2}}{\left(d^{grain}\right)^2}}}$$

$$k_2 = 0.9k_1\frac{b}{g}\left(1 - \frac{K_B T}{Db^3}\ln\left(\frac{\dot{\varepsilon}}{\dot{\varepsilon}_0}\right)\right)$$

Calibration
τ_0^s, k_1, D, g, q

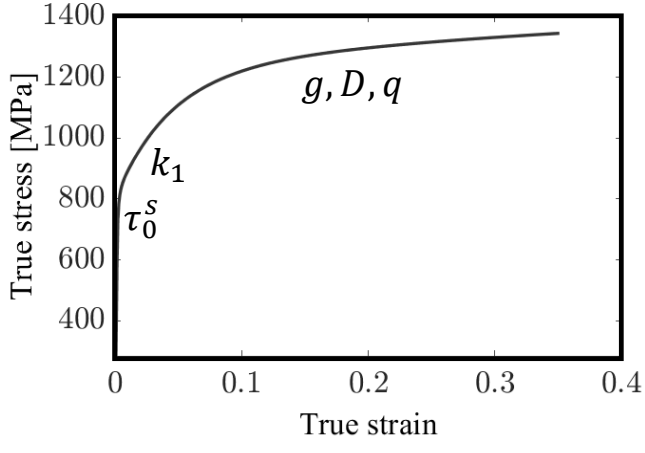

$\square^s$: *slip system*

ρ_{for}^s : *forest dislocations* [*mobile*]

ρ_{deb}^s : *debris dislocations* [*sessile*]

b : *Burgers vector*

μ : *Shear modulus*

d^{grain} : *Gr. size*

DFT-informed DD hardening

$$g = \frac{\Delta\Gamma_{SFE}}{\mu b_{\langle 11\bar{2}\rangle}} = \frac{\left|\Gamma_{USFE} - \Gamma_{ISFE}\right|}{\mu b_{\langle 11\bar{2}\rangle}}$$

Normalized activation energy

$$q = \frac{H_{Va}^F}{16\mu b_{\langle 11\bar{2}\rangle}^3 g}$$

Rate of dislocation debris

Calibration	DFT
τ_0^s, k_1, D	g, q

Γ_{USFE} : *unstable stacking fault energy*

Γ_{ISFE} : *intrisntic stacking fault energy*

H_{Va}^F : *vacancy formation energy*

DFT-Informed CPFFT

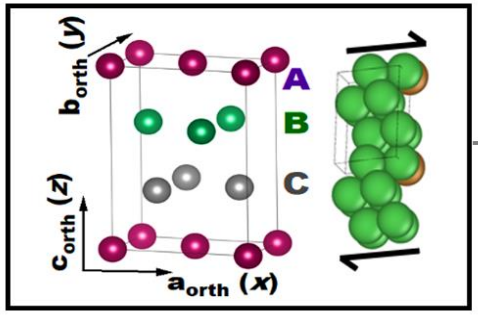

Density functional theory

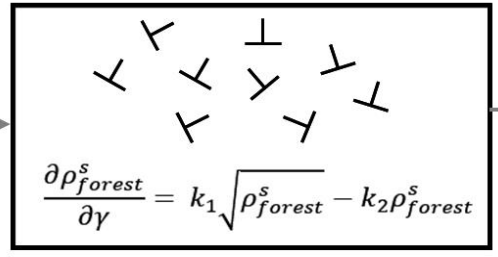

Dislocation density hardening

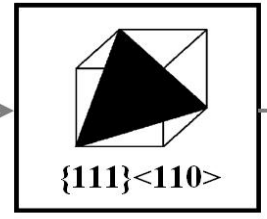

FCC slip systems

FFT voxel

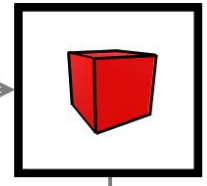

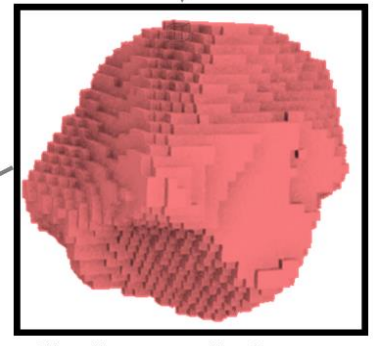

Single crystal of many voxels

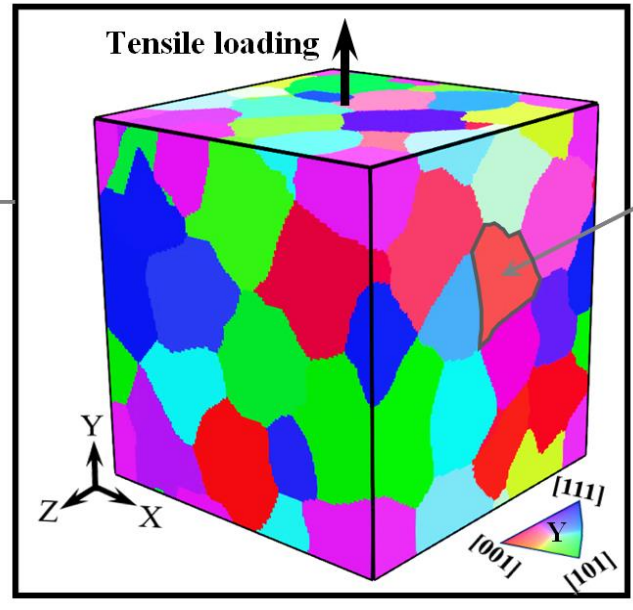

Polycrystalline deformation

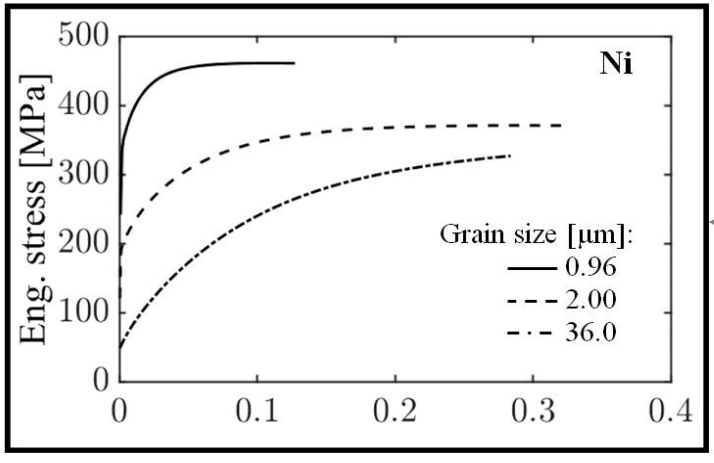

Simulation of flow response in polycrystalline Ni as a function of grain size

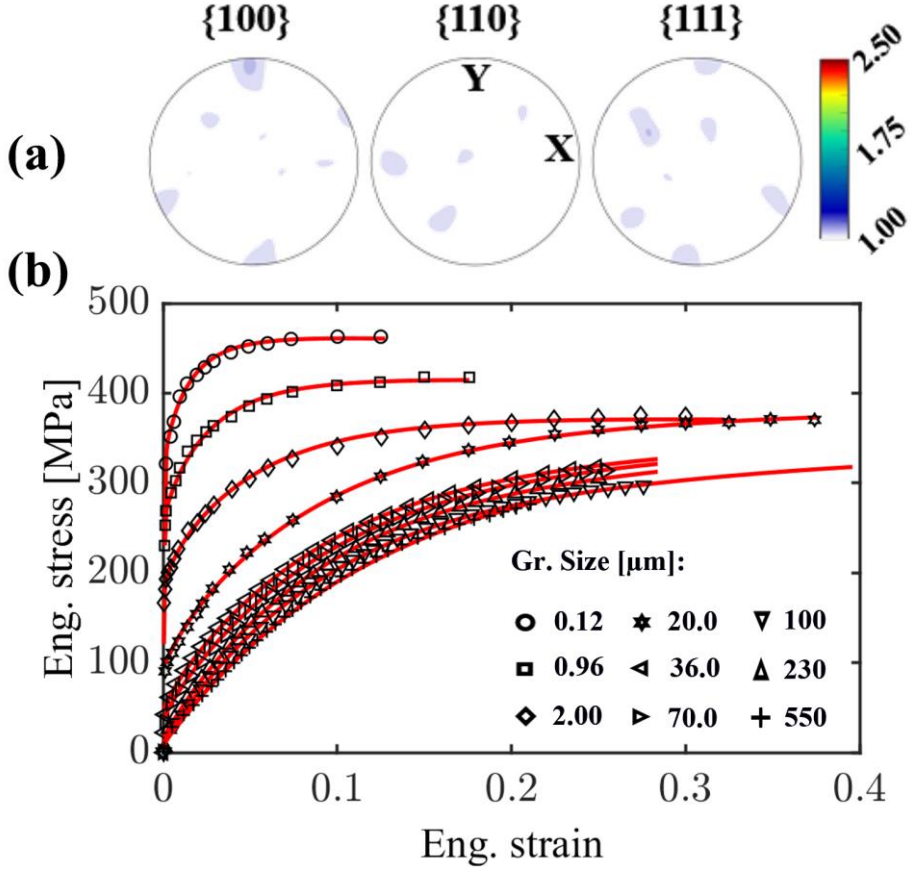

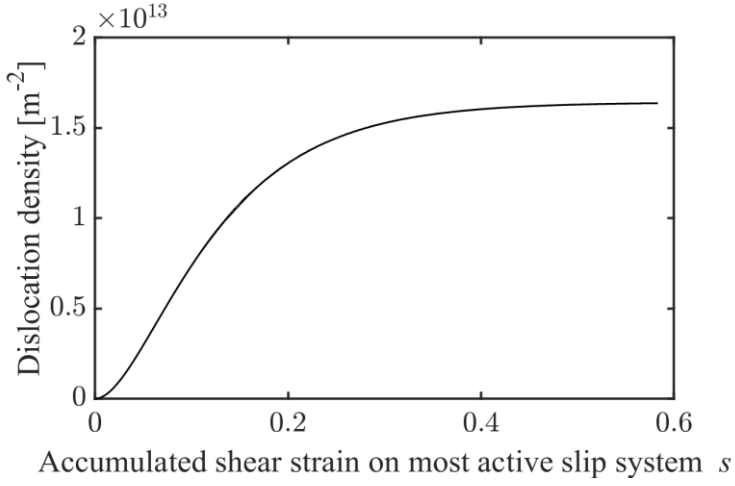

(c)

Correlating calibrated DD parameters with grain size

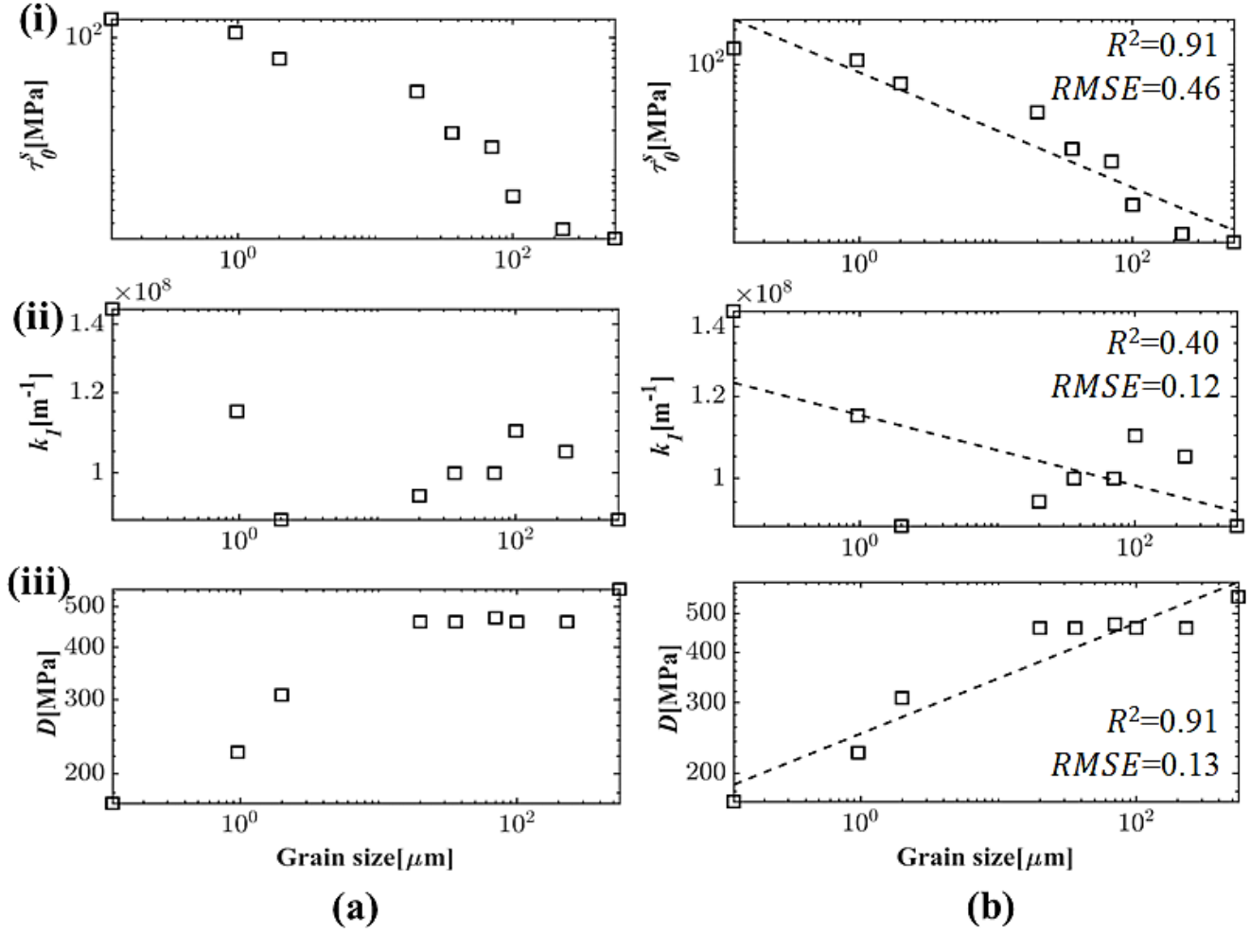

Identification of micromechanical hotspots

- Full-field CPFFT model offers **quantification of micromechanical fields**
- Provide insights into micromechanical **micro-crack incubation zones**
- Assist with **microstructure sensitive design** for performance optimization

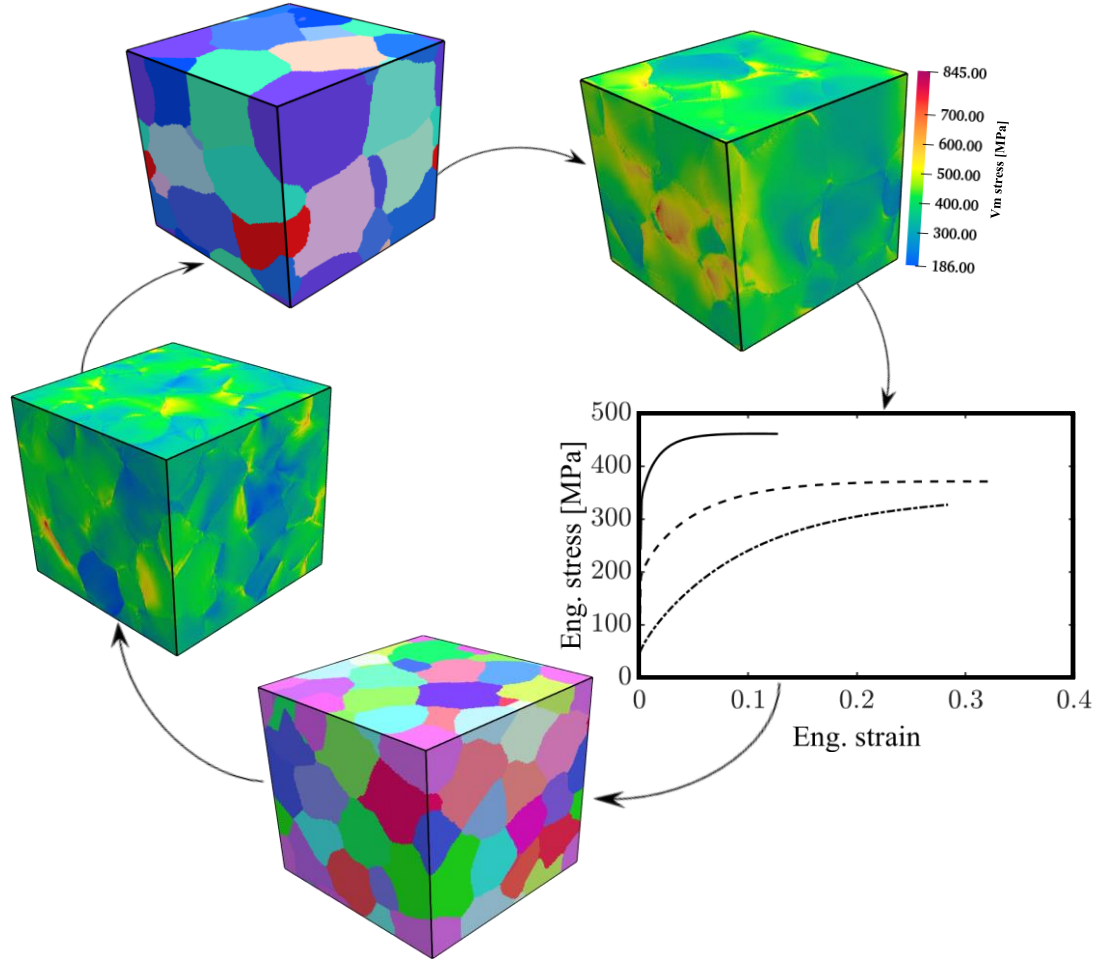

Correlation of microstructural descriptors with full-field hotspots

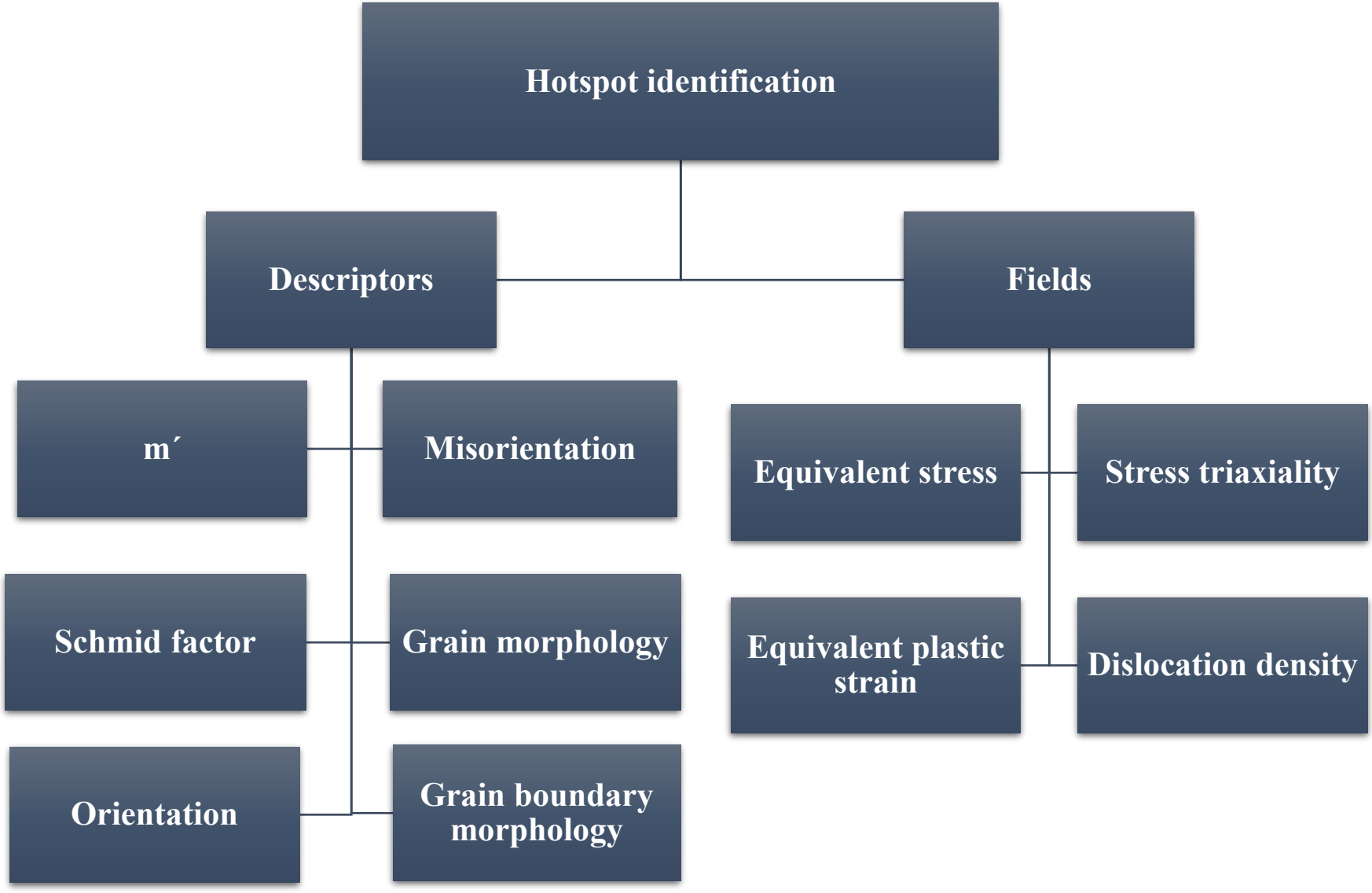

Microstructural descriptors

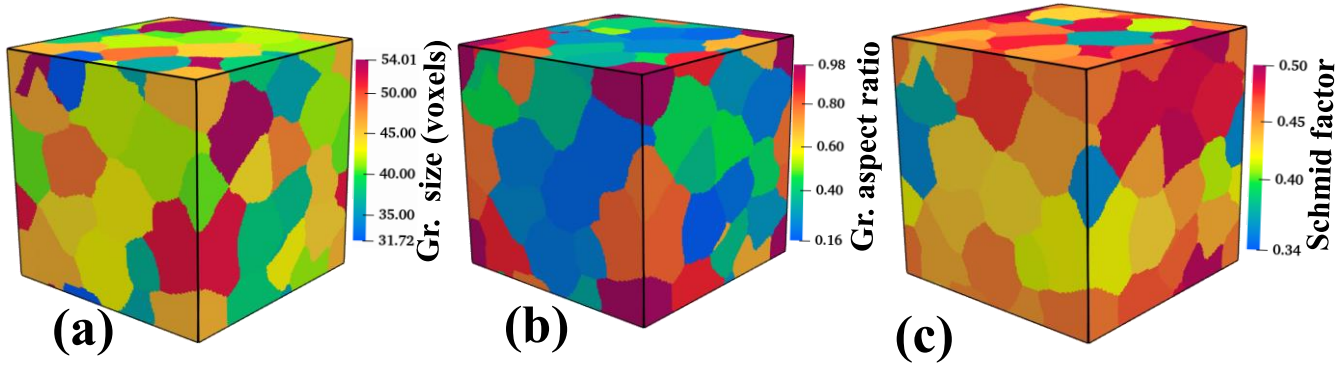

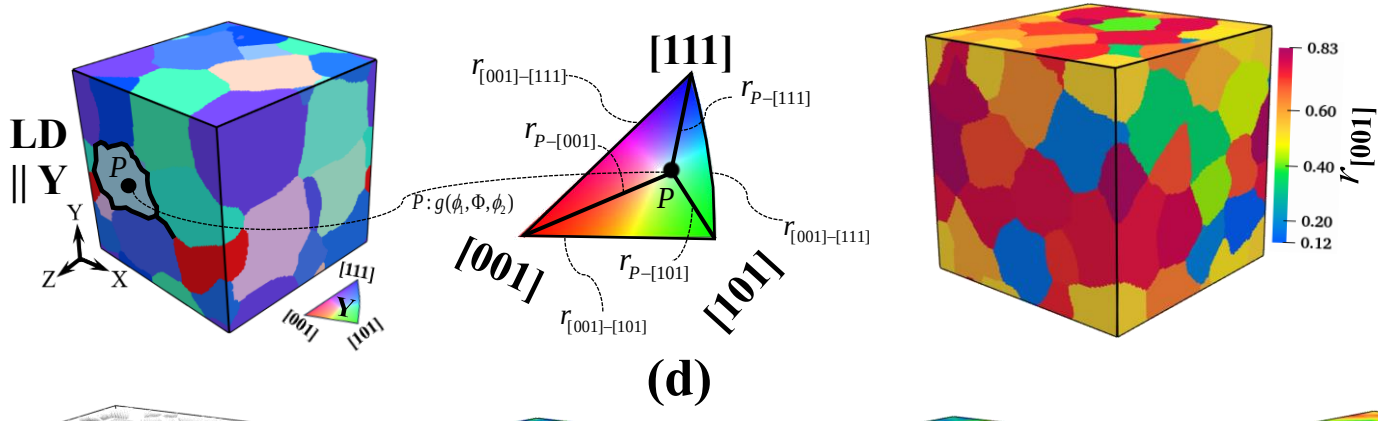

(i) GB surface
(ii) triple junction
(iii) quadruple point

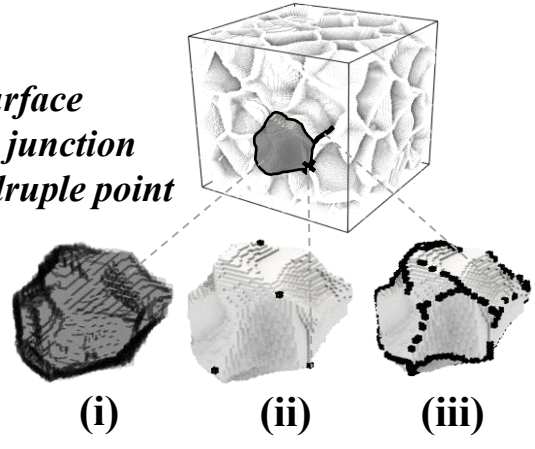

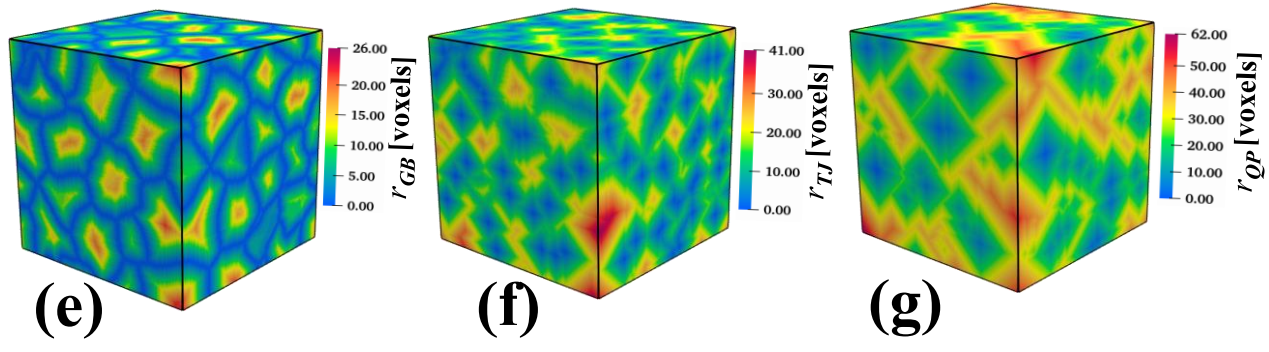

Local misorientation and m´ at grain boundary (GB)

m´ indicates the slip transmissibility at GBs

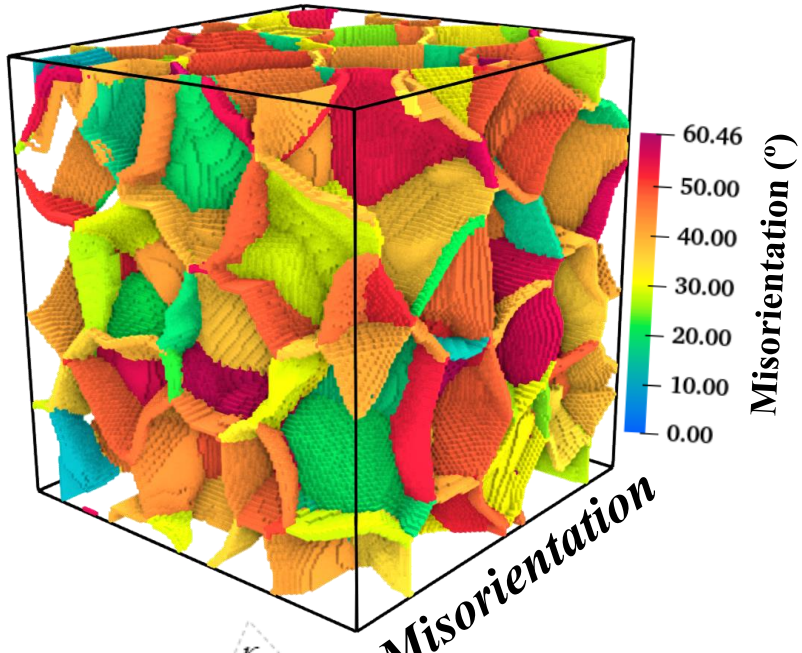

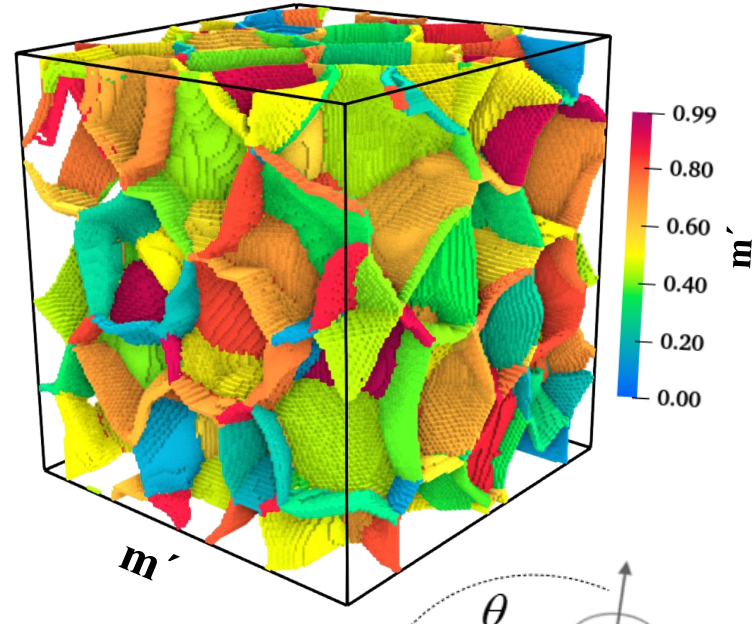

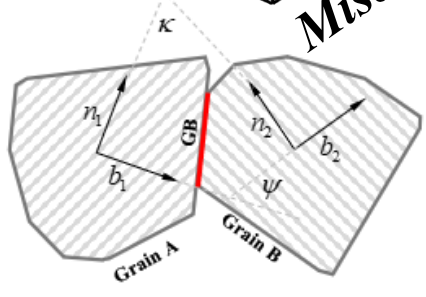

$$0 \le m' = \cos\kappa \cos\psi \le 1$$

$m' = 0 \equiv$ Impenetrable GB for slip transfer

$m' = 1 \equiv$ Slip is fully transmissible

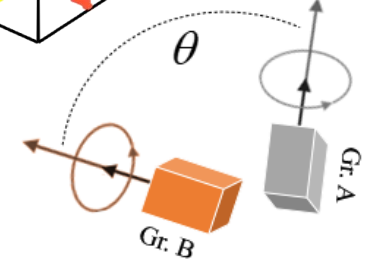

$$\theta = \cos^{-1}\left(\frac{\sum_i \Delta g_{ii}^{AB} - 1}{2}\right)$$

$$\Delta g_{ij}^{AB} = \left(g_{ij}^{A}\right)^{-1} g_{ij}^{B}$$

Grain Morphology

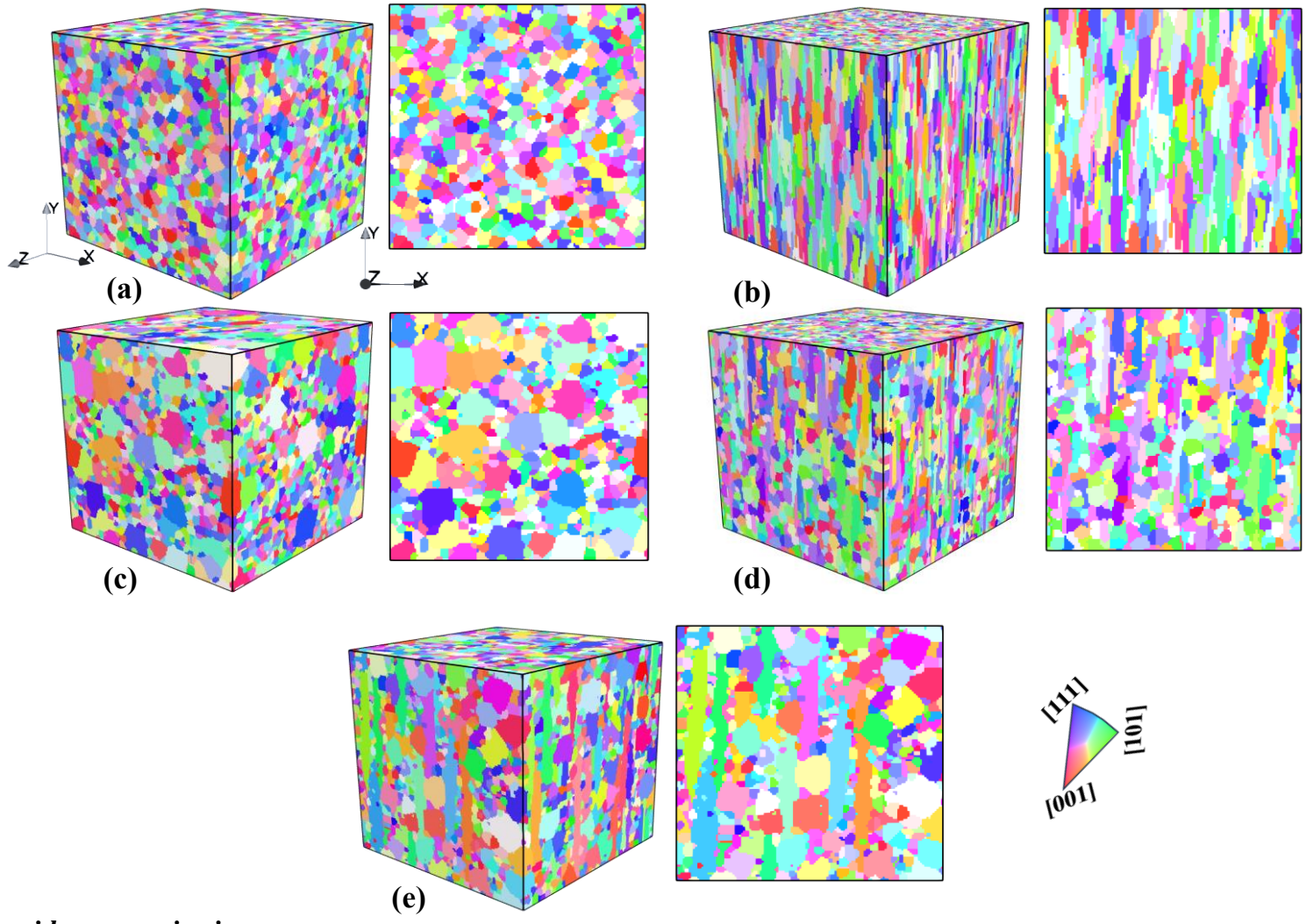

(a) equiaxed
(b) elongated
(c) equiaxed grains with contrast in size.
(d) mix of equiaxed and elongated
(e) mix of equiaxed and elongated with contrast in size and shape.

Estimating microstructural feature importance on stress hotspots using machine learning: Random forest and SHapley Additive explanation (SHAP)

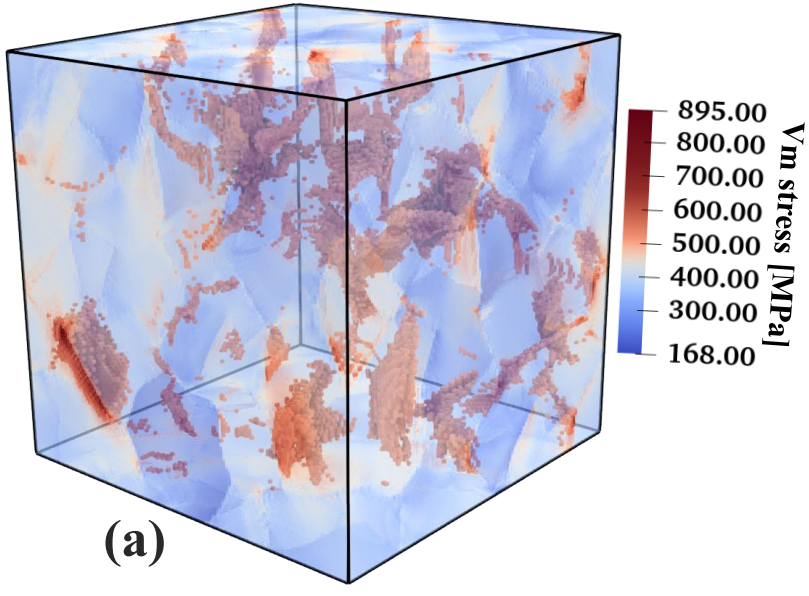

(a)

Hotspots in Ni microstructure after uniaxial deformation to 2.5% strain

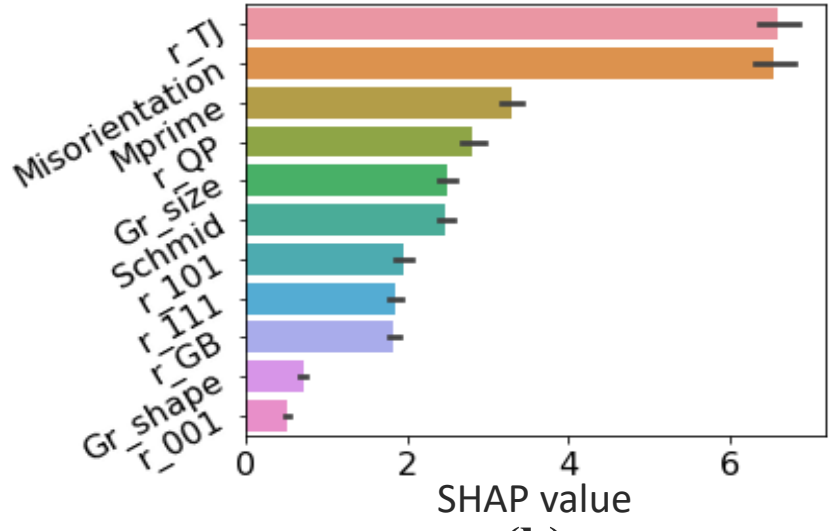

(b)

Feature importance

Summary

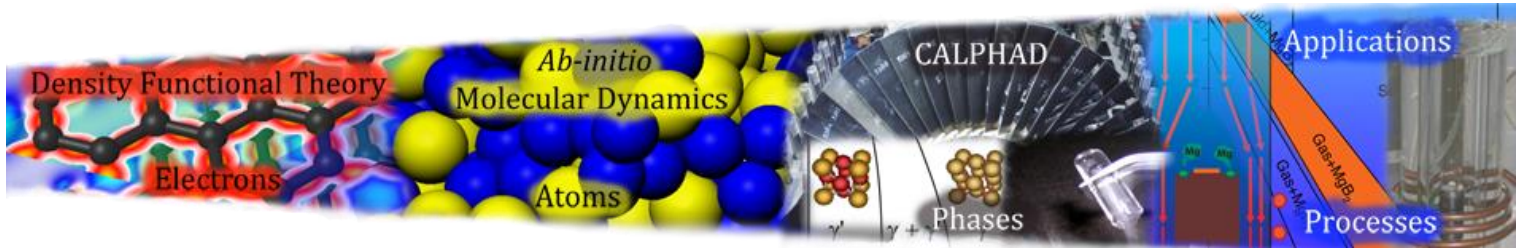

Multiscale approach from electron, atoms, to phase, and applications

- High-throughput calculations and modeling for efficient data generation
  - DFT-based first-principles calculations of thermodynamic/mechanical properties
  - Machine learning models to predict and analyze properties
  - CALPHAD modeling to develop the databases
  - Python-based open-source codes: SIPFENN, DFTTK, PyCalphad and ESPEI
- A combined DFT/CP approach to study tensile stress-stain behaviors
  - Crystal plasticity finite element method (CPFEM) for single crystals with a phenomenological hardening law (PAN)
  - Ideal shear strength of alloys, $Ni_{11}X$ and $Ni_{34}XZ$, by DFT calculations and machine learning models
  - DFT-informed hardening model based on dislocation densities, efficiently implemented through FFT for larger scale polycrystal calculations

K-fold cross-validation (KCV)

Cross-validation is a statistical technique used to evaluate the suitability of a model type.
Errors for models tested on each fold are averaged and compared across models.